

## Photoemission study of the electronic structure of $C_{60}$ and $K_x C_{60}$

M. Merkel, M. Knupfer, M. S. Golden, and J. Fink

*Kernforschungszentrum Karlsruhe, Institut für Nukleare Festkörperphysik,  
Postfach 3640, D-7500 Karlsruhe 1, Federal Republic of Germany*

R. Seemann and R. L. Johnson

*II. Institut für Experimentalphysik, Universität Hamburg, Luruper Chausee 149,  
D-2000 Hamburg 50, Federal Republic of Germany*

(Received 9 September 1992)

High-resolution photoemission studies have been performed on undoped and K-doped  $C_{60}$  films. In the undoped material, temperature-dependent measurements showed no significant change of the valence-band electronic structure on crossing the structural phase transitions at 90 K and 249 K. Studies of  $K_x C_{60}$  conducted with a variety of photon energies and doping levels show that  $K_3 C_{60}$  is a metal, with a sharp Fermi edge situated at the maximum of the occupied part of the lowest unoccupied molecular orbital-or LUMO-derived bands. The density of states observed at the Fermi level shows a maximum at  $x = 3$ , indicating that there is no pseudogap at the Fermi level of  $K_3 C_{60}$ . The spectral weight of the occupied LUMO-derived states with respect to those of the highest occupied molecular orbital (HOMO) is found to be photon-energy dependent. A surface K content greater than  $x = 6$  can be achieved and is found to be correlated with the presence of a potassium oxide overlayer. The results are discussed with reference to the need for absolute, accurate determination of the surface K content of the samples studied by photoemission.

### I. INTRODUCTION

The discovery of superconductivity in the alkali-metal-doped fullerenes,<sup>1-3</sup>  $A_3 C_{60}$  ( $A =$  mixtures of the alkali metals Na, K, Rb, and Cs), has prompted much research activity concerning the structural and physical properties of these materials. In particular, a precise knowledge of the electronic structure at and close to the Fermi level ( $E_F$ ) is fundamental to the search for the mechanism of superconductivity responsible for the high transition temperatures observed in these compounds. Photoemission provides a powerful tool for investigating the electronic structure of solids,<sup>4</sup> provided well characterized and representative surfaces of the material to be studied can be prepared. Photoemission consequently plays a major role in the study of the fullerenes.

There have been a number of studies of the occupied electronic structure of solid  $C_{60}$  in the literature.<sup>5</sup> These have revealed the remarkable nature of the electronic structure of this material, in which formation of the solid seems to have a relatively small effect on the distribution of electronic states, with a considerable degree of molecular character retained in the solid state. There is a good correlation between the main features in the experimental photoemission spectra<sup>5</sup> and the calculated electronic structure of solid  $C_{60}$ , although the experiments seemed unable to observe some of the predicted fine structure.<sup>6</sup> In particular, the degree to which the structural phase transitions<sup>7,8</sup> of solid  $C_{60}$  at 249 and 90 K effect the electronic structure has remained largely unknown, although calculations give strong evidence that the orientation of the  $C_{60}$  molecules in the solid plays an important role in the determination of the electronic structure.<sup>9</sup> To shed some light on these questions, we have recorded

temperature-dependent valence-level photoemission spectra of solid  $C_{60}$  with a total experimental energy resolution of only 25 meV. We find that the failure to observe fine structure in the electronic distribution predicted by calculation is not related to the experimental resolution, but may arise from a mixture of vibronic and correlation effects.

The previously published photoemission studies of the  $K_x C_{60}$  system have provided a wealth of information regarding the evolution of the electronic structure on K doping.<sup>10-13</sup> However, there are important differences in the conclusions drawn by the authors as regard the nature of the half-doped,  $K_3 C_{60}$  phase. Broadly speaking, of those studies which include a determination of the K content, the majority favor metallic  $K_3 C_{60}$ , with a sharp Fermi edge observed at the maximum of the occupied LUMO-derived bands in spectra of an appropriate resolution.<sup>12,14</sup> In contrast, Takahashi *et al.*<sup>15</sup> claim that  $K_3 C_{60}$  exhibits a pseudogap of about 0.5 eV at the Fermi level, due to either electron correlation or polaron formation. This claim raises fundamental questions about the role correlation plays in the electronic properties of doped  $C_{60}$ , and has been cited by Lof *et al.*<sup>15</sup> as support for their contention that stoichiometric  $K_3 C_{60}$  is a Mott-Hubbard insulator with a gap of  $\sim 0.7$  eV.

In an effort to reconcile these differences we have conducted a series of photoemission measurements on thin films of  $K_x C_{60}$ . We have measured valence-band photoemission with a wide range of photon energies, and concurrently monitored the surface stoichiometry using Mg  $K_\alpha$  x-ray photoemission spectroscopy (XPS) analysis of the K  $2p$  and C  $1s$  core levels. We find that  $K_3 C_{60}$  supports a sharp Fermi edge, situated at the maximum of the occupied LUMO-derived bands. Furthermore, the spec-

tra at each doping stage can be simulated by a superposition of appropriately weighted spectra from  $C_{60}$ ,  $K_3C_{60}$ , and  $K_6C_{60}$ , indicating the three-phase nature of the  $K_xC_{60}$  system in our samples. We also report data that have important consequences for the manner in which the surface K content can be determined, and suggest a possible cause of the discrepancy in the published results. Firstly, the spectral weight of the occupied LUMO-derived states with respect to those of the HOMO (LUMO/HOMO ratio) is dependent on the incident photon energy, although the two groups of states have nominally the same angular momentum.<sup>16</sup> Secondly, we have strong evidence that it is possible to have a surface K content significantly in excess of 6, which is linked to the presence of a surface potassium oxide species.

## II. EXPERIMENTAL

A mixture of fullerenes was synthesized by the contact-arc method<sup>17</sup> under 100 Torr of helium. After extraction with toluene,  $C_{60}$ ,  $C_{70}$ , and higher fullerenes were separated using column chromatography on neutral alumina with 5% toluene in hexane as eluant. Thin-film polycrystalline  $C_{60}$  samples (thickness  $\sim 100$  Å, as measured using a quartz-crystal thickness monitor) were prepared *in situ* on a freshly deposited gold film by evaporation of  $C_{60}$  from a clean, degassed Knudsen cell. Subsequent doping with potassium was carried out using a thoroughly degassed getter source (SAES Getters, Italy). The approximate stoichiometry of the  $K_xC_{60}$  film was controlled by monitoring the exposure time of the sample to the K flux produced at a given getter current, together with the readings from a quartz-crystal thickness monitor situated next to the sample. All samples were annealed prior to measurement at 150 °C for 30 min. The photoemission energy distribution curves (EDC's) were referenced to the position of the Fermi level of the Au substrate.

EDC's excited using synchrotron radiation, together with the unmonochromatized Mg  $K_{\alpha}$  XPS, were recorded at the Flipper II beamline<sup>18</sup> at HASYLAB, Hamburg. Electron energy analysis was carried out using a commercial double-pass cylindrical mirror analyzer. The total-energy resolution of these measurements was set between 200–400 meV for the EDC's (photon-energy dependent) and  $\sim 1.4$  eV for XPS. After  $C_{60}$  deposition, no measurable XPS signal was observed from any of the substrate levels. For each particular  $K_xC_{60}$  composition, EDC's covering both the valence band and, where possible, the K  $3p$  shallow core level, were recorded at photon energies of 20, 21.22, 65, and 110 eV, followed by XPS investigation of the C  $1s$  and K  $2p$  core levels. We emphasize that each set of measurements was performed on the same sample within a period of 2 hr, thus allowing direct comparison of the valence-level EDC data with the stoichiometry from analysis of the shallow core-level and XPS spectra. The core-level spectra were stripped of contributions from Mg  $K_{\alpha 3,4}$  satellite radiation and background subtracted following the method of Shirley.<sup>19</sup> Correction of integrated peak areas for differences in photoionization cross section<sup>20</sup> allowed determination of

the surface K/C ratio. We estimate the accuracy of this procedure to be about  $\pm 10\%$ , mainly due to the difficulty in quantifying the extended high binding-energy structure associated with the C  $1s$  core level and the applicability of atomic photoionization cross sections to the solid state.

High-resolution ultraviolet photoemission spectroscopy (UPS) data excited with HeI radiation were recorded in Karlsruhe using a commercial spectrometer (Vacuum Science Workshop, Manchester, U.K.), equipped with a 50-mm radius hemispherical analyzer. The total-energy resolution for the high-resolution photoemission was 25 meV, as determined from low-temperature measurements on a clean Au film. All results shown here have been stripped of contributions from HeI satellite radiation, in which the satellite intensities were derived from analysis of the spectrum of pure  $C_{60}$ . In this case, unambiguous determination of the satellite intensities is possible as clear structures resulting from satellite radiation stimulated photoemission from the HOMO-derived band appear in the gap.

## III. RESULTS

### A. Undoped $C_{60}$

At room temperature  $C_{60}$  adopts a face-centred-cubic (fcc) structure in which free rotation of the  $C_{60}$  molecules occurs. Near 250 K, there is a structural phase transition attributed to orientational ordering leading to a hindered rotation of the fullerene molecules, and the description of the system within a simple cubic (sc) lattice.<sup>7</sup> Below 90 K, the  $C_{60}$  molecules no longer rotate at all, although a degree of rotational disorder remains frozen into the structure.<sup>8</sup> The exact orientation of each fullerene molecule with respect to its neighbors is expected to exert a significant influence on the electronic density of states (DOS).<sup>9</sup>

High-resolution valence-band photoemission profiles of undoped  $C_{60}$  as a function of temperature can be seen in Fig. 1, together with the results of a calculation of the electronic density of states of  $C_{60}$  within the framework of the local density approximation (LDA). The valence-band UPS spectra were recorded at 300, 160, and 9 K and the LDA calculated DOS (Ref. 6) for "unidirectionally" oriented  $C_{60}$ , broadened with a Lorentzian of width 50 meV and shifted so that the onset of the HOMO is aligned with that of the experimental data. In the UPS spectra, the bands resulting from the  $\pi$ -derived HOMO ( $h_{1u}$ ), HOMO-1 ( $h_g, g_g$ ) and HOMO-2 ( $t_{2u}, g_u$ ) molecular orbitals are evident, centered at 2.3, 3.7, and 5.8 eV binding energy (BE). The HOMO-derived band has a bandwidth of  $\sim 1.1$  eV.  $\sigma$ -derived features are observed at  $\sim 5.3$  and  $\sim 7.1$  eV BE. These have a much reduced bandwidth in comparison to the  $\pi$ -derived bands, probably due to low intermolecular  $\sigma$  orbital overlap.

The good agreement between the main features of the calculation and the experimentally determined DOS can clearly be seen from Fig. 1—the relative positions and widths of the  $\pi$  bands are well reproduced, although there appears to be some underestimation of the binding energy of the  $\sigma$  states in the calculation, probably a result

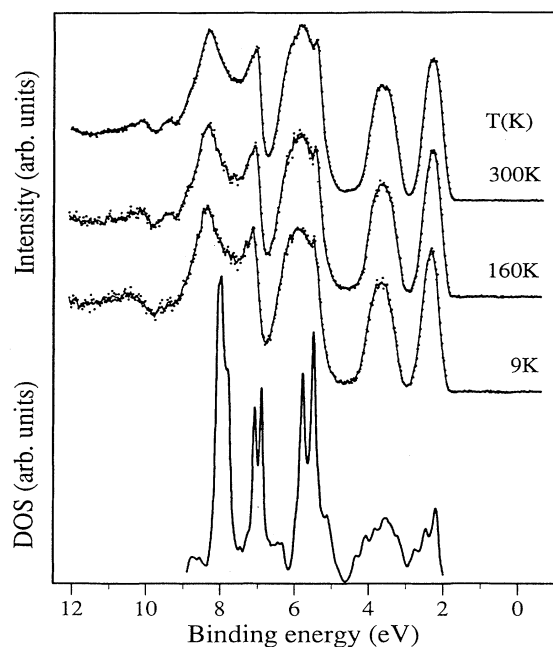


FIG. 1. Temperature-dependent high-resolution UPS spectra ( $h\nu=21.11$  eV) of pure  $C_{60}$  for sample temperatures of 300, 160, and 9 K. The raw data are shown as points, the line is intended as a guide to the eye. Shown at the bottom of the figure is the calculated valence-band DOS of unidirectionally oriented  $C_{60}$  (from Ref. 6).

of the underestimation of the  $\sigma-\sigma^*$  gap. The other discrepancy is the fine structure. For example, the calculated HOMO-derived bands have three components, split in energy by an amount an order of magnitude greater than the overall energy resolution of the UPS spectra, yet in the latter, no indication of the splitting can be seen. Similarly, despite the differences in the DOS predicted for the different orientations of  $C_{60}$  in the solid, the UPS data recorded from samples in each phase are almost indistinguishable.

### B. K-doped $C_{60}$

Valence- and core-level photoemission spectra from a series of  $K_xC_{60}$  thin films can be seen in Fig. 2. The right-hand panel shows valence-level EDC's, excited with photons of energy 65 eV, including the region of the K 3p shallow core level. XPS spectra of the C 1s and K 2p core levels recorded from the same samples are shown in the left-hand panel. The development of the structure close to the Fermi level observed in the EDC's is due to the filling of the LUMO-derived conduction bands and is clearly related to the increasing K content as seen by the growth of the K 3p level visible at 18 eV BE and the K 2p core-level spin-orbit doublet at  $\sim 294.5$  and  $\sim 297.3$  eV BE in the XPS profiles. From analysis of the XPS spectra, surface K doping levels can be assigned to the EDC's. In addition, analysis of the intensity of the K 3p

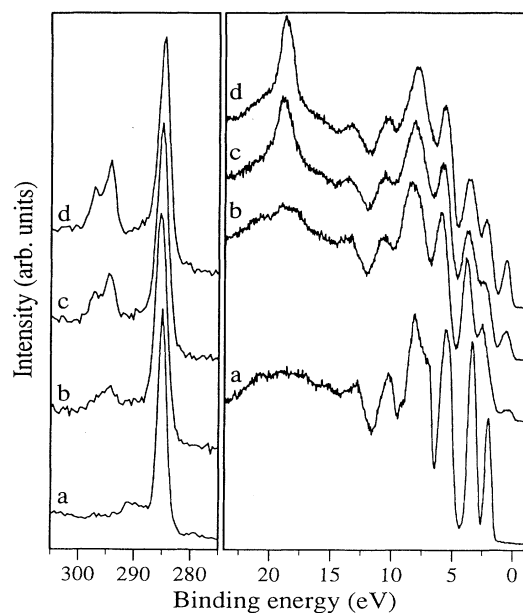


FIG. 2. Right-hand panel: EDC's of  $K_xC_{60}$  recorded with  $h\nu=65$  eV. Left-hand panel: Mg  $K_\alpha$  XPS recorded from the same samples showing the C 1s core level at  $\sim 285$  eV BE and the K 2p doublet centered at  $\sim 296$  eV BE. Samples (a), (b), (c), and (d) have  $x$  values of 0, 2.3, 4.3, and 6.3, respectively, determined from analysis of the XPS spectra shown on the left. Note the states near  $E_F$  increasing in tandem with the K 3p shallow core level seen at 18 eV BE in the right-hand panel.

shallow core level is in keeping with the absolute K determination from the XPS data. As can be seen from Fig. 2, during the series of experiments recorded at the synchrotron, the exact composition  $K_3C_{60}$  was not achieved—the closest composition being  $x=2.3$ . Nevertheless, careful inspection of the region near the Fermi level reveals that this composition of  $K_{2.3}C_{60}$  does support a Fermi edge.

The structure of the electronic states close to  $E_F$  as a function of doping can be seen more clearly in Fig. 3. These spectra were recorded at high resolution using a HeI discharge lamp. The  $x$  values were determined by comparison of the LUMO/HOMO ratio with that of the samples measured at HASYLAB with the same photon energy, for which an absolute determination of the surface K content is possible from the XPS analysis. In this case, the stoichiometry  $K_{3.1}C_{60}$  was reached, which represents half-doping, within the experimental uncertainty. The question of phase purity of films grown in the manner described here will be discussed later.

In Fig. 3, the occupied LUMO-derived states have been expanded by a factor of 3, and clearly show a density of states at  $E_F$  for all compositions other than  $x=0$  and 6, with a sharp Fermi edge visible for  $4.4 > x > 1.9$ . There is no indication, within our resolution, of a pseudogap for samples close to, or at  $x=3$ —the maximum of the spectral weight of the LUMO-derived bands is at  $E_F$

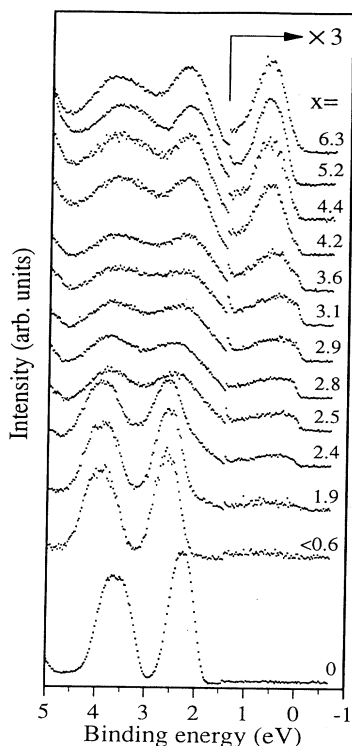


FIG. 3. Room-temperature high-resolution He I photoemission spectra of  $K_x C_{60}$  as a function of K doping level,  $x$ . The occupied part of the LUMO-derived bands is expanded vertically by a factor of 3. Spectra are normalized to the area of the HOMO-derived feature and stripped of contributions from satellite radiation.

for this stoichiometry. The compositions around half-doping also show considerable broadening of the HOMO and HOMO-1 peaks, which has been suggested to be due to a combination of both many-body and phonon contributions.<sup>21</sup> A significant feature to note from Fig. 3 is that the states induced upon K doping are not rigid-band-like: The separation of the maxima of the HOMO and the LUMO in  $C_{60}$  is at least 2.3 eV (the BE of the HOMO), however, in the fully doped,  $K_6 C_{60}$ , the separation of the HOMO-1 and HOMO bands is reduced to 1.7 eV. The observed width of the conduction band at room temperature remains virtually unchanged, from the very first stages of doping until  $K_6 C_{60}$  is reached. The spectra for each doping level can be synthesized by superposition of appropriately weighted spectra of  $C_{60}$ ,  $K_3 C_{60}$ , and  $K_6 C_{60}$ , although the quality of the fit is reduced for doping levels  $x < 1$ . For example, the double-peak structure observed in the occupied LUMO-derived bands of  $K_{3.6} C_{60}$  in Fig. 3 is a result of the superposition of contributions from the occupied LUMO-derived bands of  $K_3 C_{60}$  and  $K_6 C_{60}$  and as such can be accurately fitted with a sum of the spectra from  $K_3 C_{60}$  and  $K_6 C_{60}$ , taken in the ratio 4:1, respectively. This is further evidence for the existence of only three stable phases in the  $K_x C_{60}$  system<sup>22-24</sup> under the growth conditions used here.

The development of the magnitude of the DOS at  $E_F$

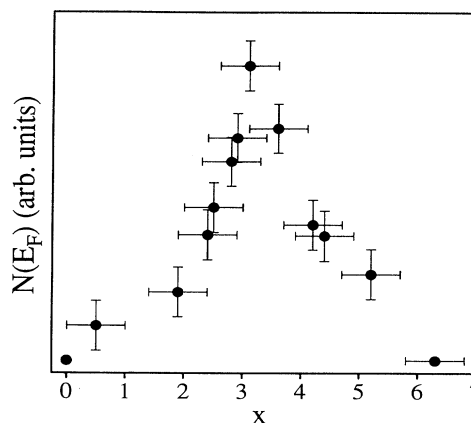


FIG. 4. The size of the DOS at  $E_F$  as a function of  $x$  for  $K_x C_{60}$ , determined from the height of the Fermi edges observed in the spectra of Fig. 3.

as a function of K doping level can be seen in Fig. 4. Here the height of the Fermi-Dirac cutoff seen in the data of Fig. 3, normalized to the intensity of the HOMO-derived states, is plotted against the absolute surface K doping level. Within the experimental uncertainty, the maximum DOS at  $E_F$  is found in the half-doped,  $K_3 C_{60}$ . It should be noted that at half-doping, the Fermi level is situated at the maximum of the occupied part of the LUMO-derived states (see Fig. 3). Whether or not such a sample is 100% phase-pure  $K_3 C_{60}$  is difficult to determine. Scanning tunneling microscope studies of fulleride films grown under different conditions on a variety of substrates indicate that the fulleride films grown in the manner described here may have a grain size of only 80 Å and more recent attempts to grow highly ordered films have met with some success, although ordered films of phase-pure  $K_3 C_{60}$  remain difficult to achieve.<sup>25</sup>

The LUMO of  $C_{60}$  is threefold degenerate and the intensity of this feature (normalized to the fivefold degenerate HOMO) has been used in the past as a method of quantifying the degree of alkali-metal doping in photoemission studies of the  $A_x C_{60}$  materials. In the course of our measurements at different photon energies, we found that the experimentally measured ratio of the intensity of the LUMO-derived bands to HOMO-derived bands (denoted LUMO/HOMO ratio) changes as a function of photon energy for a given K-doping level. The valence-band photoemission profiles of the HOMO-1, HOMO, and LUMO-derived bands of a representative sample ( $K_{4.3} C_{60}$ ) are shown in Fig. 5. These were recorded at the synchrotron with photon energies of 20, 21.22, 65, and 110 eV. The inset to Fig. 5 shows the LUMO/HOMO ratio for each K doping level, including  $x = 4.3$ , determined by a peak fitting procedure, as a function of the energy of the exciting radiation. The change of the LUMO/HOMO ratio as a function of the photon energy can be seen from Fig. 5, in  $x = 4.3$  having a maximum at  $h\nu = 65$  eV, for the photon energies used in this study. This trend holds for the other compositions studied, with the LUMO/HOMO ratio being slightly reduced at

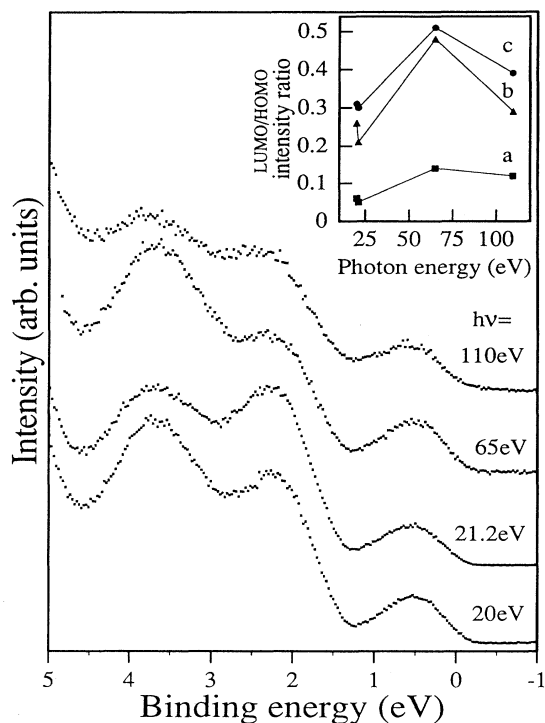


FIG. 5. Synchrotron radiation photoemission spectra of  $K_{4.3}C_{60}$ , recorded with the incident photon energy as shown. The inset shows the LUMO/HOMO ratios determined from peak fitting of spectra from films of composition (a)  $x=2.3$ , (b)  $x=4.3$ , and (c)  $x=6.3$ , as a function of photon energy.

$h\nu=21.22$  eV in comparison with 20 eV, at a maximum for 65 eV and at an intermediate value for 110 eV (see the inset to Fig. 5). This result has important consequences for the comparison of doping levels determined from the LUMO/HOMO ratio between studies carried out with different photon energies, and is discussed more fully later.

In Fig. 6, the valence-level photoemission spectrum of  $K_{6.3}C_{60}$  is shown together with that of a film with an absolute potassium stoichiometry, as determined from *in situ* XPS, of  $K_{11.5}C_{60}$ . Both spectra were recorded with a photon energy of 65 eV, and include the K  $3p$  shallow core level at 18 eV BE. Within experimental error, the  $K_{6.3}C_{60}$  spectrum represents the signature of pure, fully doped  $K_6C_{60}$ . The lower trace is the result of subtracting the  $K_6C_{60}$  spectrum from that of the  $K_{11.5}C_{60}$  after normalizing the two spectra in the region between the K  $3p$  shallow core level and the bulk of the valence-band structure (i.e., at about 15 eV BE—similar results are achieved by normalizing to the HOMO) and shifting the spectrum of  $K_6C_{60}$  to higher BE by 0.45 eV, so that the occupied part of the LUMO in the two spectra is aligned. The exact position of the Fermi level in both  $K_6C_{60}$  and the overdoped material depends on pinning by states situated in the gap between the fully occupied LUMO (the HOMO of  $K_6C_{60}$ ) and the former LUMO+1

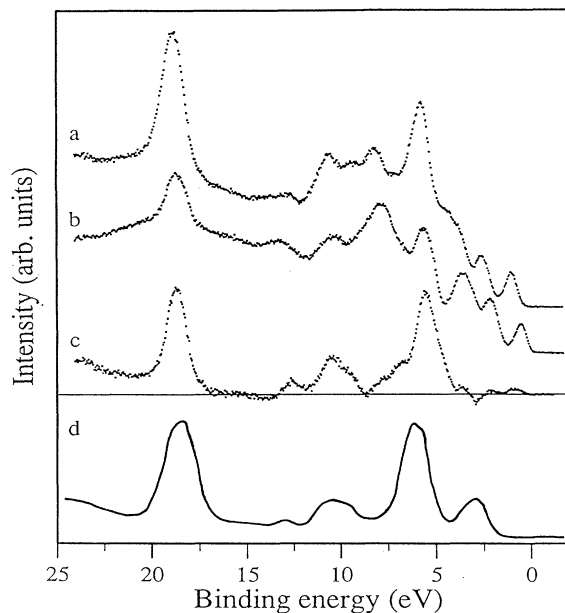


FIG. 6. Synchrotron radiation photoemission spectra of (a)  $K_{11.5}C_{60}$  and (b)  $K_{6.3}C_{60}$ , recorded with a photon energy of 65 eV. The lower trace, (c), shows the result of subtracting curve (b) from curve (a) after shifting the former by 0.45 eV to higher BE so that the LUMO's of the two spectra are aligned. A zero line is drawn through the difference spectrum. Shown for comparison, curve (d) is photoemission data recorded at 35 K from an oxygen-exposed K film with a photon energy of 80 eV, taken from Ref. 26.

(now the LUMO of  $K_6C_{60}$ ). However, to determine the binding-energy positions of any extra contributions in the overdoped spectrum, the  $K_6C_{60}$  spectrum was shifted prior to the subtraction, so that the spectral features of the fulleride line up. It is evident from the subtraction spectrum that there is not only the expected extra K  $3p$  intensity in the spectrum of the overdoped material, but that there is also significant intensity concentrated in three peaks centered at  $\sim 5.5$ , 10, and 12.5 eV BE. Comparison of these features with the photoemission spectra of a potassium film exposed to oxygen, recorded at 35 K with a photon energy of 80 eV by Qiu *et al.*<sup>26</sup> shown at the bottom of Fig. 6, reveals that they are of the correct energy and relative intensity to be due to the valence levels of oxygen in a potassium oxide species. The peak observed at lower BE (2.9 eV) by Qiu *et al.* is attributed to photoemission from the  $2p$  valence levels of  $O^{2-}$  ions buried beneath a K metal surface layer (this interpretation is based on an analogous feature observed in the oxidation of Cs metal<sup>31</sup>). The efficient screening by the metal overlayer results in the low BE of this peak. As we do not have a metallic K overlayer in the overdoped sample, this highly screened O  $2p$  valence emission is not observed in Fig. 6(c). It should be noted that at no stage were any signs of oxide contamination observed for samples with  $x$  values of less than 6.

#### IV. DISCUSSION

##### A. Undoped $C_{60}$

The time scale of the photoemission experiment is such that it records a "snapshot" of the electronic structure relevant to a particular rotational orientation of the  $C_{60}$  molecules in the solid.<sup>27</sup> However, the UPS data is also a spatial average over  $\sim 1 \text{ mm}^2$  of the sample surface and therefore the spectra recorded at 300 and 160 K shown in Fig. 1 will represent a sum of contributions from different  $C_{60}$  orientations. Below 90 K, 80% of the  $C_{60}$  molecules in the solid have been estimated from neutron-scattering measurements to be orientationally ordered,<sup>8</sup> with the remaining 20% distributed between a number of different orientations. Thus, the photoemission data recorded at 9 K will also represent a sum over a number of orientations, although the relative proportions of the orientations will be different to that observed at higher temperatures. Consequently, if no other broadening mechanism is involved, the predominantly ordered low-temperature phase would be expected to give rise to a different DOS than that of the more orientationally disordered sc and fcc phases. Figure 1 shows that this is not observed in the experiment. This is not a result of the experimental energy resolution, as the differences in the calculated DOS (Ref. 9) are much greater than 25 meV. Possible causes for the absence of such fine structure in the experimental spectra include the excitation of phonons, Jahn-Teller splitting in the positive  $C_{60}$  ion in the photoemission final state or broadening due to the existence of satellites resulting from the effects of strong correlation.

Measurements of gas phase  $C_{60}$  show that the line due to the molecular  $h_{1u}$  (HOMO) state has a width of about 0.3 eV, with a shoulder to higher binding energy consistent with transitions within the vibrational manifold of the positive ion.<sup>28</sup> Thus it is reasonable to suggest that there is a contribution from vibronic broadening in the solid state. The question of the magnitude of the correlation energy, and consequently its effect on the electronic structure of undoped and doped  $C_{60}$  continues to provoke vigorous debate. By comparison of high-resolution x-ray excited Auger spectra with a self-convolution of valence-level photoemission data, Lof *et al.*<sup>15</sup> conclude that  $U$  (intramolecular) is of the order of 1.6 eV for undoped  $C_{60}$ . Analogous measurements by Brühwiler *et al.*<sup>29</sup> have suggested a  $U$  value of 1.2 eV. Others have argued that taking into account the magnitude of the interaction with the nearest neighbor  $C_{60}$  molecules, the apparent correlation effects may not be very much greater than the bandwidth.<sup>21</sup>

At this stage it is difficult to assess the exact contribution of correlation effects to the observed width of the bands in photoemission of undoped  $C_{60}$ . Suffice to say that the width of the features in the experimental photoemission spectra may be composed of contributions from both band formation, excitation of intramolecular vibrations,<sup>21</sup> and electron correlation. The combined effect of these broadening mechanisms may be to smear out the changes in the electronic DOS predicted to result from

the rotational orientation accompanying the phase transitions at  $\sim 250$  and 90 K.

##### B. $K_x C_{60}$

###### 1. Effects of K doping

The effects of K doping on the valence levels of  $C_{60}$  are shown in both Figs. 2 and 3. The progressive occupation of the LUMO can clearly be seen as the K doping level increases. The spectra around half-doping are considerably broadened in both the LUMO- and HOMO-derived bands. This broadening could result from a number of sources, including a lifting of the degeneracy of the molecular-like levels as a function of the filling of the LUMO as a consequence of a Jahn-Teller-type distortion of the C atoms in the  $C_{60}$  framework. The occupied part of the LUMO is also remarkably wide, even at the lowest K doping levels. LDA band-structure calculations predict an occupied LUMO with width of the order of 0.3 eV in the half-doped material.<sup>6</sup> It can be seen from Figs. 2 and 3 that the width of the occupied LUMO-derived band remains almost constant at about 1.5 eV, regardless of the K doping level. This width may be caused by excitation of phonons during photoemission or the effects of strong coupling between the half-filled LUMO-derived band and the phonons, observed in Raman scattering<sup>23</sup> and predicted by theory.<sup>30</sup> As has already been mentioned, the significant reduction in the HOMO-LUMO separation from  $C_{60}$  to the HOMO-1-HOMO separation in  $K_6C_{60}$ , is a strong indication of the importance of non-rigid-band behavior upon doping.

###### 2. Is there a pseudogap at $E_F$ in $K_3C_{60}$ ?

The valence-band photoemission spectra shown in Fig. 2 closely resemble those of Benning *et al.*<sup>14</sup> also recorded with a photon energy of 65 eV. Spectra we recorded from the same samples with  $h\nu = 110$  eV (not shown) are equally in agreement with those of Chen *et al.*<sup>12</sup> However, there appear to be some discrepancies between our data and those of Takahashi *et al.*<sup>13</sup> These differences, and the reasons put forward to explain them, warrant discussion, as the possible observation of a pseudogap at the Fermi level of a system, which in the bulk resembles a good metal and is a superconductor, is of considerable importance.

Our spectra recorded at the same photon energy as Takahashi *et al.* (20 eV) show no signs of a pseudogap at the Fermi level for the doping level  $x = 2.3$  (the nearest composition to  $K_3C_{60}$  achieved at the synchrotron). We note that the strict phase separation observed in our photoemission data means that the Fermi edge observed for the sample of composition  $K_{2.3}C_{60}$  can be due solely to  $K_3C_{60}$ . In their paper,<sup>13</sup> Takahashi *et al.* discussed the differences between the data sets published at that time. They suggested that the differences between their work and that of Chen *et al.*<sup>12</sup> could be explained by variation in cross section resulting from the different photon energies used in the two experiments. By using photon energies equivalent to those used by Takahashi *et al.*<sup>13</sup> (20

eV), Benning *et al.*<sup>14</sup> (65 eV), and Chen *et al.*<sup>12</sup> (110 eV) we are able to state categorically that the appearance of an alleged pseudogap at  $E_F$  for  $x \sim 3$  does not depend on the incident photon energy used in the photoemission experiment. In contrast, we agree with the statement of Takahashi *et al.* that a likely cause of the discrepancy between their data and that of other groups lies in the actual composition of the samples studied by photoemission.

Takahashi *et al.*<sup>13</sup> used three methods for the determination of the K doping level. The reading from a thickness monitor, a conductivity measurement on a reference sample and the intensity of the K 3*p* shallow core level observed in the photoemission experiment. Although useful as a rough guide, a thickness monitor cannot be used as an accurate method of calibrating the real K content of the film under scrutiny. The intensity of the K 3*p* peak can only give the *relative* K content, relying on the designation of one spectrum to a particular  $x$  value. Lastly, the composition monitored by the *in situ* conductivity determination is that of an unannealed, and hence possibly inhomogeneous,  $K_xC_{60}$  film different from the one used for photoemission. It should be noted that the depthscale of the doping probed by the photoemission and the conductivity measurement is very different. In addition, it has been shown that the resistivity of  $K_xC_{60}$  films changes only very slightly between  $x$  values of around 1.5–5, as monitored by photoemission.<sup>14</sup> Consequently, given these caveats, and in the light of the photoemission spectra of  $K_xC_{60}$  we have recorded with the same photon energy, we believe it is quite possible that the photoemission spectrum shown as that of  $K_3C_{60}$  given in Ref. 13 in fact represents that of a much higher K doping level, and that the true spectral profile of  $K_3C_{60}$ , or compositions very close to half-doping, is shown in Fig. 3 (labeled  $x = 3.1$ ), in which the Fermi level cuts the maximum of the occupied LUMO-derived bands. This conclusion, together with the maximum in the DOS at  $E_F$  observed for  $x = 3$  (see Fig. 4), enables us to state with confidence that there is no pseudogap at the Fermi level of  $K_3C_{60}$  within an energy scale equal to our resolution of 25 meV. Although the existence of a Mott-Hubbard insulator with a gap of 0.7 eV for ordered material with *exactly*  $x = 3$  cannot be ruled out,<sup>15</sup> the data presented here suggest that this eventuality is unlikely.

### 3. Photon-energy dependent HOMO / LUMO ratio

At first glance the modulation of the HOMO/LUMO ratio as a function of the incident photon energy is an intriguing result. In alkali-metal-doped  $C_{60}$ , the HOMO and LUMO bands are derived from the  $h_{1u}$  and  $t_{1u}$  molecular orbital (MO's) of the undoped fullerene. Both these MO's correspond to spherical harmonics with  $l = 5$ , and so in the simplest picture of the photoemission process, their photoionization cross sections should behave similarly with changing photon energy. For most materials, if such intensity modulations occurred only for low photon energies ( $h\nu < 25$  eV), then they could be understood in terms of the effect of the final density of states on

the photoemission spectrum. At these photon energies, the photoemission spectrum represents the mapping of the initial DOS onto the final DOS via an appropriate matrix element, and is described in terms of the so-called energy distribution of the joint density of states.<sup>4</sup> At higher photon energies, the final density of states usually contains less structure, and is assumed to be almost free-electron like. In this case, the photoemission spectrum reflects primarily the matrix-element weighted occupied DOS.

This free-electron-like behavior of the higher energy final DOS appears not to apply in the case of  $C_{60}$ , where from synchrotron radiation photoemission measurements it has been proposed that there are significant differences in the final states of different parity, even up to energies of the order of 100 eV.<sup>5</sup> Although the parity of the LUMO- and HOMO-derived bands of doped  $C_{60}$  is the same, the symmetry of these bands is different and thus it is possible that the photon-energy dependent changes in the LUMO/HOMO ratio are a result of different energy dependent structure in the unoccupied DOS of different symmetry, leading to nonequivalent matrix elements for photoemission from the LUMO- and HOMO-derived bands.

It should be noted that the effective escape depth of the photoelectrons also varies as a function of their kinetic energy, although accurate values of the inelastic mean free path as a function of kinetic energy are not available for  $K_xC_{60}$ . The highly approximate nature of the so-called universal curve means that extreme caution should be exercised in interpreting these LUMO intensity changes solely in terms of changing inelastic mean free path. In addition, there is no evidence for a difference between the surface and the bulk at these doping levels.

### 4. Surface potassium oxide species in $K_xC_{60}$ with $x > 6$

The data shown in Fig. 6 graphically illustrate the potential problems encountered when dealing with such a reactive dopant as potassium. Although the UHV conditions used in such sample preparation procedures, and the purity of the alkali-metal flux from the SAES getter source are usually assumed to be such that no contamination problems can occur, Fig. 6 shows that this situation cannot always be taken for granted. In this case, an overlayer of a potassium oxide is formed such that the XPS analysis gives an absolute composition of  $K_{11.5}C_{60}$ . It should be noted that the more surface sensitive measurement of the K 3*p* shallow core level (with  $h\nu = 65$  eV), gives a still higher K content, consistent with the surface nature of this oxide overlayer.

There are two potential sources of oxygen-related contamination. Firstly, contamination of the residual vacuum with oxygen-containing species. Observation of the mass spectrum of the residual gas of a well-maintained UHV system will yield partial pressures of water or oxygen of the order of  $10^{-13}$  mbar or less. However, during operation of a Knudsen cell or SAES getter, it is conceiv-



able that this value may increase sharply. We have found that during operation of a *thoroughly degassed* SAES getter source, the partial pressure of water does increase significantly above the background level, as monitored by *in situ* quadrupole mass spectroscopic measurements. A second potential source of contamination is the  $C_{60}$  itself. Raman measurements<sup>23</sup> have indicated the possibility of the existence of oxygen contamination of  $C_{60}$  prepared in the standard manner. Whether this contamination remains to a high enough degree in a sample of  $C_{60}$  repeatedly cycled at elevated temperature under UHV conditions is a moot point. We note that only after the formation of fully doped  $K_6C_{60}$ , was there any contribution from  $KO_x$  species, suggesting that only when there is no possibility of the potassium being involved in the formation of the energetically highly stable fulleride, does it reside at the surface in its elemental state for an adequate length of time to react with oxygen containing species in the residual vacuum. We reiterate that no traces of oxide contamination were observed for samples of stoichiometry  $x < 6$ .

The observation of such a surface over doping resulting from oxide formation has important consequences for the estimation of the real K doping level in the fulleride if absolute determination of the K stoichiometry is unavailable, and may result in spectra such as that shown for  $K_{11.5}C_{60}$  being assigned to fully doped  $K_6C_{60}$ . This fact, taken together with the photon-energy dependence of the occupied LUMO intensity at a given doping level, means that great care should be taken in the determination of the alkali-metal doping level in these fullerides and the comparison of data recorded with different experimental conditions.

## V. SUMMARY

It has been shown that the valence-band electronic structure of  $K_xC_{60}$  can be probed in detail using high-

resolution photoemission. The main features of the experimentally determined valence band of  $C_{60}$  are well reproduced by calculation. The changes predicted in the occupied DOS of the undoped material, as a result of rotational ordering accompanying the phase transitions at 90 and  $\sim 250$  K, are not observed in temperature-dependent UPS measurements. Possible reasons for the failure to observe any temperature dependence include broadening of the experimental structure due to phonon excitation during photoemission, Jahn-Teller-like distortion resulting from strong electron-phonon coupling or the effects of electronic correlation.

On doping with K, the occupied DOS is seen to change, with the appearance of a new band, derived of occupied LUMO states, near the Fermi level. The maximum of this band is cut by the Fermi level in  $K_3C_{60}$ , which supports the largest DOS at  $E_F$  in the  $K_xC_{60}$  series. There is no evidence for the existence of a pseudogap at the Fermi level of the half-doped material. The photoemission spectra show signs of strong non-rigid-band behavior on doping. The photon-energy dependence of the observed LUMO intensity and the existence of an over-doped surface layer associated with a potassium oxide species have important consequences for the accurate determination of the absolute surface alkali-metal doping level in electron spectroscopic studies of the fullerides.

## ACKNOWLEDGMENTS

We are indebted to V. P. Antropov for provision of the calculated DOS appearing in Fig. 1 and to E. Sohmen for the preparation of  $C_{60}$ . M.S.G. is grateful for financial support from SERC and NATO. This work was in part supported by the Bundesminister für Forschung und Technologie (BMFT) under project No. 05 5GUABI.

- <sup>1</sup>A. F. Hebard, M. J. Rosseinsky, R. C. Haddon, D. W. Murphy, S. H. Glarum, T. T. M. Palstra, A. P. Ramirez, and A. R. Kortan, *Nature (London)* **350**, 600 (1991).
- <sup>2</sup>M. J. Rosseinsky, A. P. Ramirez, S. H. Glarum, D. W. Murphy, R. C. Haddon, A. F. Hebard, T. T. M. Palstra, A. R. Kortan, S. M. Zahurak, and A. V. Makhija, *Phys. Rev. Lett.* **66**, 2830 (1991); K. Holzer, O. Klein, S.-M. Huang, R. B. Kaner, K.-J. Fu, R. L. Whetten, and F. Diederich, *Science* **252**, 1154 (1991).
- <sup>3</sup>K. Tanigaki, T. W. Ebbesen, S. Saito, J. Misuki, J. S. Tsai, Y. Kubo, and S. Kuroshima, *Nature (London)* **352**, 222 (1991).
- <sup>4</sup>See, for example, *Photoemission in Solids I and II*, edited by M. Cardona and L. Ley, (Springer-Verlag, Berlin, 1978).
- <sup>5</sup>J. H. Weaver, J. L. Martins, T. Komeda, Y. Chen, T. R. Ohno, G. H. Kroll, N. Troullier, R. E. Haufler, and R. E. Smalley, *Phys. Rev. Lett.* **66**, 1741 (1991); P. J. Benning, D. M. Poirier, N. Troullier, J. L. Martins, J. H. Weaver, L. P. F. Chibante, and R. E. Smalley, *Phys. Rev. B* **44**, 1962 (1991); D. L. Lichtenberger, K. W. Nebesny, C. D. Ray, D. R. Huffman,

- and R. D. Lamb, *Chem. Phys. Lett.* **176**, 203 (1991).
- <sup>6</sup>S. Satpathy, V. P. Antropov, O. K. Andersen, O. Jepsen, O. Gunnarsson, and A. I. Lichtenstein, *Phys. Rev. B* **46**, 1773 (1992); (private communication).
- <sup>7</sup>P. A. Heiney, J. E. Fischer, A. R. McGhie, W. J. Romanow, A. M. Denenstein, J. P. McCauley, Jr., A. B. Smith III, and D. E. Cox, *Phys. Rev. Lett.* **66**, 2830 (1991).
- <sup>8</sup>W. I. F. David, R. M. Ibbertson, T. J. S. Dennis, J. P. Hare, and K. Prassides, *Europhys. Lett.* **18**, 219 (1992).
- <sup>9</sup>O. Gunnarsson, S. Satpathy, O. Jepsen, and O. K. Andersen, *Phys. Rev. Lett.* **67**, 3002 (1991).
- <sup>10</sup>P. J. Benning, J. L. Martins, J. H. Weaver, L. P. F. Chibante, and R. E. Smalley, *Science* **252**, 1417 (1991); for a review of the Minnesota group's work see, J. H. Weaver, *Acc. Chem. Res.* **25**, 143 (1992) and J. H. Weaver, *J. Phys. Chem. Solids* (to be published).
- <sup>11</sup>G. K. Wertheim, J. E. Rowe, D. N. E. Buchanan, E. E. Chaban, A. F. Hebard, A. R. Kortan, A. V. Makhija, and R. C. Haddon, *Science* **252**, 1419 (1991).



- <sup>12</sup>C. T. Chen, L. H. Tjeng, P. Rudolf, G. Meigs, J. E. Rowe, J. Chen, J. P. McCauley, A. B. Smith, A. R. McGhie, W. J. Romanow, and E. W. Plummer, *Nature (London)* **352**, 603 (1991).
- <sup>13</sup>T. Takahashi, S. Suzuki, T. Morikawa, H. Katayama-Yoshida, S. Hasegawa, H. Inokuchi, K. Seki, K. Kikuchi, S. Suzuki, K. Ikemoto, and Y. Achiba, *Phys. Rev. Lett.* **68**, 1232 (1992).
- <sup>14</sup>P. J. Benning, D. M. Poirier, T. R. Ohno, Y. Chen, M. B. Jost, F. Stepaniak, G. H. Kroll, J. H. Weaver, J. Fure, and R. E. Smalley, *Phys. Rev. B* **45**, 6899 (1992).
- <sup>15</sup>R. W. Lof, M. A. von Veenendaal, B. Koopmans, H. T. Jonkman, and G. A. Sawatzky, *Phys. Rev. Lett.* **68**, 3924 (1992).
- <sup>16</sup>See, for example, S. Saito and A. Oshima, *Phys. Rev. Lett.* **66**, 2637 (1991).
- <sup>17</sup>W. Krätschmer, L. D. Lamb, K. Fostiropoulos, and D. R. Huffman, *Nature (London)* **347**, 354 (1990).
- <sup>18</sup>R. L. Johnson and J. Reichardt, *Nucl. Instrum. Methods* **208**, 791 (1983).
- <sup>19</sup>D. A. Shirley, *Phys. Rev. B* **5**, 4709 (1972).
- <sup>20</sup>J. J. Yeh and I. Lindau, *At. Data Nucl. Data Tables* **32**, 1 (1985).
- <sup>21</sup>V. P. Antropov, O. Gunnarsson, and O. Jepsen, *Phys. Rev. B* **46**, 13 647 (1992).
- <sup>22</sup>D. M. Poirier, T. R. Ohno, G. H. Kroll, Y. Chen, P. J. Benning, J. H. Weaver, L. P. F. Chibante, and R. E. Smalley, *Science* **253**, 646 (1991).
- <sup>23</sup>T. Pichler, M. Matus, J. Kürti, and H. Kuzmany, *Phys. Rev. B* **45**, 13 841 (1992).
- <sup>24</sup>R. M. Fleming, M. J. Rosseinsky, A. P. Ramirez, D. W. Murphy, J. C. Tully, R. C. Haddon, T. Siegrist, R. Tycko, S. H. Glarum, P. Marsh, G. Dabbagh, S. M. Zahurak, A. V. Mahija, and C. Hampton, *Nature (London)* **352**, 701 (1991).
- <sup>25</sup>J. H. Weaver (private communication).
- <sup>26</sup>S. L. Qiu, C. L. Lin, J. Chen, and Myron Strongin, *Phys. Rev. B* **41**, 7467 (1990).
- <sup>27</sup>The so-called “hole switch-on time” is of the order of at most  $10^{-14}$  s for photoemission with these final state energies. See, J. W. Gadzuk, in *Photoemission and the Electronic Properties of Surfaces*, edited by B. Feuerbacher, B. Fitton, and R. F. Willis (Wiley, New York, 1978).
- <sup>28</sup>D. L. Lichtenberger, M. E. Jatcko, K. W. Nebesny, C. D. Ray, D. R. Huffman, and R. D. Lamb, in *Clusters and Cluster-Assembled Materials*, edited by R. S. Averback, J. Bernholc, and D. L. Nelson, MRS Symposia Proceedings No. 206 (Materials Research Society, Pittsburgh, 1991), p. 673.
- <sup>29</sup>P. A. Brühwiler, A. J. Maxwell, A. Nilsson, R. L. Whetten and N. Mårtensson (unpublished).
- <sup>30</sup>H. Scherrer and G. Stollhoff (unpublished).
- <sup>31</sup>B. Woratschek, W. Sesselman, J. Küppers, and G. Ertl, *J. Chem. Phys.* **86**, 2411 (1987).